PERGAMON

Materials Science in Semiconductor Processing 3 (2000) 487–491

MATERIALS SCIENCE IN SEMICONDUCTOR PROCESSING

Transmission of a microcavity structure in a two-dimensional photonic crystal based on macroporous silicon

A. Birner[a,e,*], A.-P. Li[a], F. Müller[a], U. Gösele[a], P. Kramper[b], V. Sandoghdar[b], J. Mlynek[b], K. Busch[c], V. Lehmann[d]

[a] *Max-Planck-Institute of Microstructure Physics, Weinberg 2, D-06120 Halle, Germany*
[b] *Universität Konstanz, Fakultät für Physik, Universitätsstraße 10, D-78457 Konstanz, Germany*
[c] *Institut für Theorie der Kondensierten Materie, Physikhochhaus, Universität Karlsruhe, D-76128 Karlsruhe, Germany*
[d] *Infineon Technologies AG Corp. Technol., Otto-Hahn-Ring 6, D-81730 München, Germany*
[e] *Infineon Technologies, Memory Products, D-01099 Dresden, Germany*

Abstract

Photonic crystals consist of regularly arranged dielectric scatterers of dimensions on a wavelength scale, exhibiting band gaps for photons, analogous to the case of electrons in semiconductors. Using electrochemical pore formation in n-type silicon, we fabricated photonic crystals consisting of air cylinders in silicon. The starting positions of the pores were photolithographically pre-defined to form a hexagonal lattice of $a = 1.58\,\mu m$. The photonic crystal was microstructured to make the photonic lattice accessible for optical characterization. Samples with different filling factors were fabricated to verify the gap map of electric and magnetic modes using Fourier-transform infrared (IR) spectroscopy. The complete band gap could be tuned from 3.3 to 4.3 μm wavelength. We were able to embed defects such as waveguide structures or microcavities by omitting certain pores. We carried out transmission measurements using a tunable mid-IR optical parametric oscillator. The resonance is compared with theoretical expectations.

Keywords: Photonic crystal; Two-dimensional; Infrared; Complete band gap; Transmission; Microcavity

1. Introduction

Dielectric structures with periodicities of their dielectric constant on a wavelength scale are capable of exhibiting complete photonic band gaps (PBGs). This fact generated much attention in the last decade [1–5]. Several recipes were given to form two- [6,7] and three-dimensional photonic crystals [8–10] working in the (near) infrared or visible spectral range and providing complete band gaps, at least in principle. To reach the abundant field of applications and enhanced devices by exploiting the novel properties of photonic crystals [11–17], precise experimental studies of, e.g., wave-propagation behavior in photonic crystals are indispensible. For the detailed optical characterization of PBG materials, macroporous silicon turned out to be a valuable approach, as for its fabrication, standard semiconductor processes can be made use of and thus, high geometric accuracies can be achieved. Furthermore, large-area ordered arrays of pores with high aspect ratios can be grown. For characterizations with the help of external light beams, transmission cross sections in the order of $10^4\,\mu m^2$ allow for signal intensities well above the noise, also for low brilliant, i.e. thermal light sources like the globar of our Fourier-transform-infrared (FT-IR) spectrometer.

In this paper we report the transmission behavior of hexagonal lattices of macropores in silicon with lattice constants of 1.58 μm and of an embedded microcavity structure.

*Corresponding author.
E-mail address: albert.birner@infineon.com (A. Birner).

1369-8001/00/$ - see front matter
PII: S1369-8001(00)00092-5

2. Sample preparation

First, we want to give a very brief description of the formation process of macropores in silicon, which is a particular mechanism of generation of porous silicon [19]. The details of the process can be found in [20–22]. Macropores with pore radii of several 10 μm down to fractions of 1 μm are formed, e.g. in moderately doped (1 0 0)-oriented n-type silicon wafers if anodized in an aqueous hydrofluoric acid solution and illuminated from the wafer backside. The porosity at the front of pore growth is proportional to the illumination density.

If applied to a polished silicon wafer the pore arrangement becomes random. We created pore nuclei arranged in a two-dimensional (2D), triangular lattice by lithography and alkaline etching. When the pore formation was started, the macropores inherited the hexagonal order of the nuclei to form cylindrical pores of radius $r = 0.45\,\mu m$ and a length of typically 100 μm arranged in a 2D hexagonal lattice of lattice constant $a = 1.58\,\mu m$ (cf. Fig. 1). After the pore formation, the radius r of the pores was adjusted via oxidation and subsequent removal of silicon oxide to match demanded porosity conditions.

With the help of the microstructuring technique described in [23], we created bars of macroporous silicon which allow to couple in light perpendicular to the pore axes. Fig. 1 shows thin bars of PBG material mechanically stabilized with the help of major blocks of the same material. The thickness of these bars could be adjusted by the photolithography used in the microstructuring technique to create bars of certain numbers of pore layers, down to one single layer.

3. Fourier-transform-IR measurements

For the FT-IR spectroscopic transmission measurements, a set of samples of equidistant r/a parameters, $0.36 < r/a < 0.49$, crystal orientations in the Γ–K as well as Γ–M directions and a constant number of 13 crystal

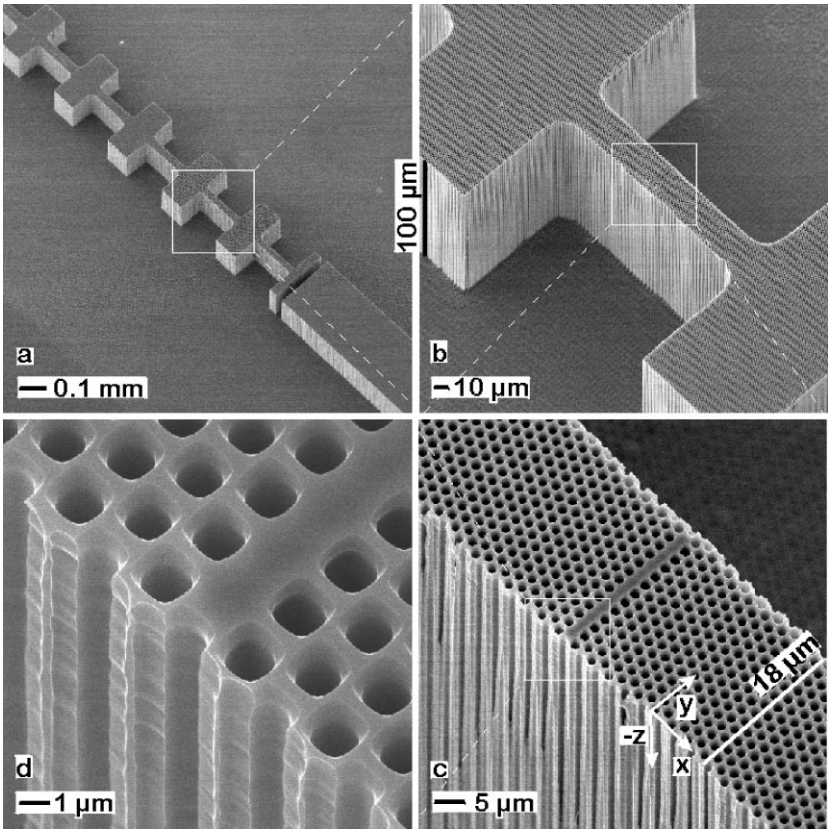

Fig. 1. Scanning electron microscope image of a bar of macroporous silicon the lateral thickness of which is periodically altered. The thinner parts consist of distinct numbers of crystal rows whereas the thicker ones provide mechanical stability (a). The wall which is marked by the square consists of 13 crystal rows (bi-layers) along the Γ–K direction of the hexagonal lattice. The height of the porous structure, which is fixed on a substrate of silicon, is 100 μm (b). By omitting some of the pores, defect structures of various geometries can be introduced (c). Cutting along the Γ–M direction provides side walls with a grating-like surface (d).

rows along several millimeters of bar length were prepared.

Contrary to Fig. 1, the specimens did not contain any defect structures. Specimens of approximately $10 \times 1\,\mathrm{mm}^2$ were cut out of the wafer and mounted between two blade-like holders, the upper one of which was placed on the top of the thin porous bar to block leakage light. The cleaved facets were screened with silver paint. The samples are probed in a mid-infrared FT-IR spectrometer with a globar light source, and a liquid-nitrogen-cooled MCT detector with its electronic band gap at $700\,\mathrm{cm}^{-1}$.

In Fig. 2, polarization-dependent transmission spectra of signal dynamics up to three orders of magnitude are shown. The measured band edges coincide well with transmission calculations analogous to [15]. The interval of the complete gap is 2900–$3300\,\mathrm{cm}^{-1}$(3.44–3.03 μm wavelength). The low offset signal within the band gaps shows a systematic increase towards higher frequencies, the cause of which is not yet well understood. In our calculation, the influence of the grating-like surface of the side walls was not taken into account. Besides this detail, the structures are very close to the theoretical model and e.g. the micro-roughness of the inner surfaces of the pores is well below $\lambda/50$. Therefore, contributions of diffusive scattering mechanisms are unlikely. This hypothesis is strengthened by the occurrence of Fabry–Perot-like resonances, which were found in the spectral ranges of high transmission close to the band edges. They become obvious only if plotted on a linear scale. A detailed analysis of these resonances will be given elsewhere.

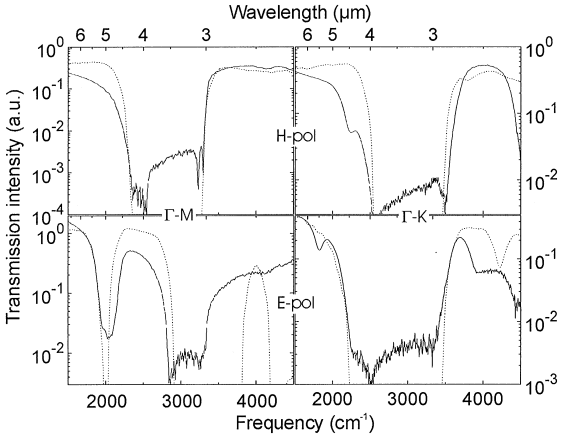

Fig. 2. Infrared transmission spectra (solid lines) and transmission calculations (dotted curves) for the Γ–K and Γ–M directions of a PBG bar ($r/a \approx 0.46$, $a = 1.5\,\mu\mathrm{m}$) consisting of 13 crystal rows. The shapes of the spectra and the band edges match well. The center of the complete gap (relative width of 12.9%) is positioned at 3.22 μm wavelength. The signal within the gap is reduced by up to three orders of magnitude.

An experimental verification of the theoretically well-known gap map [18,24] of hexagonally ordered air cylinders in a dielectric material is presented in Fig. 3. The band edges of both polarizations coincide very well with the calculations for $r/a < 0.45$. For higher porosity, the valence band edge of H modes appears to be slightly lower. More obvious are the deviations of the conduction band edge of E modes. For $0.46 < r/a < 0.48$ the signal intensity for E-pol and Γ–K was close to zero, although a transmission signal was expected. Therefore, the experimentally determined band-edge position was dominated by that of Γ–M and therefore appeared at probably very high frequencies. A narrow gap for E-modes was verified around $r/a = 0.4$ for higher bands.

4. Measurements at microcavity structure with optical parametric oscillator (OPO)

As already mentioned above, various kinds of defects could be integrated in the bars of PBG material. Figs. 1 and 4 show two kinds of structures, which were created by omitting a series of pores. The defect structures locally break the translational symmetry of the photonic crystal and create electromagnetic modes which extend through the photonic crystal at frequencies forbidden in the crystal itself. As a result, a line of defects can have the function of a waveguide. Single defects provide localized electromagnetic modes analogous to the modes of microcavities. In addition to conventional cavities, localization in two or three dimensions becomes possible. The first demonstration of a waveguide microcavity at near-IR frequencies was presented in [25]. Our approach was to integrate a microcavity in a 2D PBG structure.

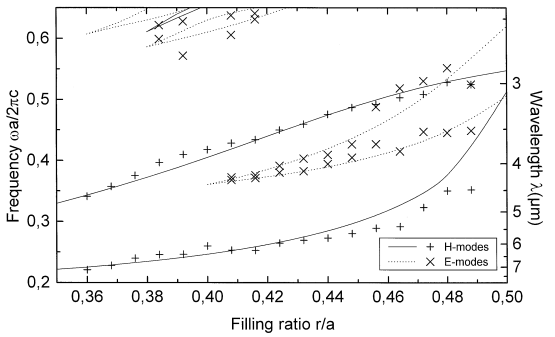

Fig. 3. Gap map of a 2D photonic crystal of air cylinders in silicon. Band edges of a set of specimens of equidistant filling ratio r/a were determined using FT-IR spectroscopy. The crosses represent the measured data whereas the lines are calculated using a plane wave expansion method. The frequency space in between two crosses of the same type indicates the interval of the photonic band gap for the corresponding light polarization.

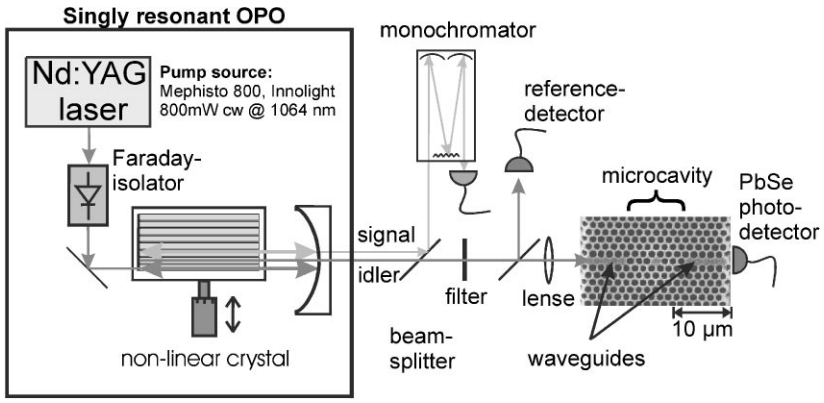

Fig. 4. Setup of optical parametric oscillator (OPO) with the use of which integrated waveguide-like structures could be investigated. The active medium of the OPO cavity is a chip of periodically poled $LiNbO_3$ offering a set of different period lengths [26]. Thus, signal and idler beams covered a large spectral range from 1.5 to 2.0 µm (signal) and 4.0 to 2.3 µm (idler) wavelength. A top-view image of a microcavity sample is used to illustrate the experiment.

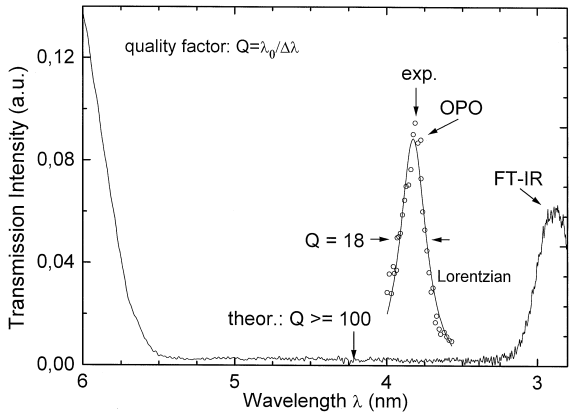

Fig. 5. Measurement of the transmission function of a microcavity structure, embedded in a 2D photonic crystal. The tunability range of the OPO is insufficient to cover the whole band gap. Therefore, an FT-IR spectrum is plotted as a reference. The resonance was found centered at a wavelength of 3.8 µm. The Q-factor of the resonance, was 18, whereas a factor of more than 100 was expected. The calculated center wavelength was deviated by 10% from the experimental data.

A sketch of the OPO setup is presented in Fig. 4. Detailed information about the setup were published in [26]. For the transmission in the mid-IR spectral range, the idler beam was used. The wavelength of the signal beam was measured with a monochromator. As the sum of idler and signal frequency equals the pump frequency the idler wavelength could be calculated easily. For focusing, spherical lenses made of sapphire were used. The filter blocked pump and signal beams. A PbSe diode was used as a photodetector (Fig. 5).

We found a resonance at a wavelength of 3.8 µm. The measured data was fit by a Lorentzian. Its Q-factor was 18, less than 20% of the expectation. One explanation of this deviation might be given by the inappropriate mode-matching conditions, as after the spherical lenses the mode in free space does not fit the vertically extended geometry of the waveguide. As a next step we try to use cylindrical lenses, made of CaF_2, to circumvent this problem.

5. Summary

We fabricated 2D photonic crystals based on macroporous silicon. The samples were microstructured to enable optical characterization. In the FT-IR transmission measurements a complete photonic band gap was found, the signal dynamic of which was up to three orders of magnitude. We verified the gap map and performed IR transmission studies of a microcavity structure embedded in a 2D photonic crystal for the first time, to our knowledge.

Acknowledgements

The authors appreciate the help by Pierre Villeneuve (MIT Cambridge, USA) and Stefan Ottow (Infineon Technologies, Dresden, Germany).

References

[1] Yablonovitch E. Phys Rev Lett 1987;58:2059.
[2] John S. Phys Rev Lett 1987;58:2486.
[3] Yablonovitch E. J Opt Soc Am B 1993;10:283.

[4] Soukoulis CM editor. Photonic band gap materials. Dordrecht: Kluwer Academic Publishers, 1996.
[5] Busch K, John S. Phys Rev E 1998;58:3896.
[6] Grüning U, Lehmann V, Ottow S, Busch K. Appl Phys Lett 1996;68:747.
[7] Knight JC, Broeng J, Birks TA, Russell PStJ. Science 1998;282:1476.
[8] Bogomolov VN, Gaponenko SV, Germanenko IN, Kapitanov AM, Petrov EP, Gaponenko NV, Prokofiev AV, Ponyavina AN, Silvanovitch NI, Smoilovitch SM. Phys Rev E 1997;55:7619.
[9] Wijnhoven JEGJ, Vos WL. Science 1998;281:802.
[10] Lin SY, Fleming JG, Hetherington DL, Smith BK, Biswas R, Ho KM, Sigalas MM, Zubrzycki W, Kurtz SR, Bur J. Nature 1998;394:251.
[11] John S, Wang J. Phys Rev Lett 1990;64:2418.
[12] Yablonovitch E. J Mod Opt 1994;41:173.
[13] Cheng SD, Biswas R, Özbay E, McCalmont JS, Tuttle G, Ho K-M. Appl Phys Lett 1995; 67:3399.
[14] Mekis A, Chen JC, Kurland I, Fan S, Villeneuve PR, Joannopoulos JD. Phys Rev Lett 1996;77:3787.
[15] Sakoda K, Ohtaka K. Phys Rev B 1996;54:5742.
[16] John S, Quang T. Phys Rev Lett 1997;78:1888.
[17] Aközbek N, John S. Phys Rev E 1998;57:2287.
[18] Villeneuve PR, Piche M. Phys Rev B 1992;46:4969.
[19] Lehmann V, Gösele U. Appl Phys Lett 1991;58:856.
[20] Lehmann V. J Electrochem Soc 1993;140:2836.
[21] Birner A, Grüning U, Ottow S, et al. Phys Stat Sol A 1998;165:111.
[22] Rönnebeck S, Carstensen J, Ottow S, Föll H. Electrochem Solid-State Lett 1999;2:126.
[23] Ottow S, Lehmann V, Föll H. J Electrochem Soc 1996;143:385.
[24] Meade RD, Brommer KD, Rappe AM, Joannopoulos JD. Appl Phys Lett 1992;61:495.
[25] Foresi JS, et al. Nature 1997;390:143.
[26] Schneider K, et al. Opt Lett 1997;22:1293.